SHORT-TERM RETRIEVAL OF WATER TRANSPARENCY FROM A CAGED-FISH FARM USING LANDSAT-8/OLI IMAGES

Ana Carolina Campos Gomes[1], Rodrigo Pentean[1,2], Jorge Laço Portinho[1], Luiz Eduardo Vicente[1], Luciana Spinelli-Araujo[1], Celso Manzatto[1], Daniel Gomes[1], Enner Alcântara[3]

[1] EMBRAPA Environment, Brazilian Corporation of Agricultural Research, Jaguariúna – SP, Brazil
[2] Pontifical Catholic University of Campinas, Campinas – SP, Brazil
E-mails: {camposgomes.ac; digobpc; jorgeportinho}@gmail.com; {luiz.vicente; luciana.spinelli; celso.manzatto; daniel.gomes}@embrapa.br
[3] São Paulo State University, Department of Environmental Engineering, São José dos Campos – SP, Brazil
E-mail: enner.alcantara@unesp.br

ABSTRACT

The intense growth of fish farming in Brazil requires an operational monitoring of water quality. Water transparency is an important parameter to investigate the biological balance in productive waters. Empirical algorithms based on remotely sensed data can be used to monitoring the spatial and temporal variability in such productive system. This work aimed to map the water transparency in caged-fish farm from space and to evaluate the short-term impact of this activity on eutrophication. The results showed that the empirical algorithm (band ratio 443/665 nm) was satisfactory for study area (MAPE = 17.5%) and the water transparency was an indicator of algal presence in fish farms.

Key words — fish farming, monitoring, water transparency, empirical model, inland water.

1. INTRODUCTION

The aquaculture increased 123% between the years of 2005 and 2015 and it is being highlighted as one of the fastest growing production activities in Brazil [1]. Among the aquaculture, the fish farming comprises 84% of the national production, mainly in inland waters, and Brazil is one of the 25 great producers, with annual yield of 562.2 thousand of tons [2, 3]. In 2016, São Paulo state was considered the third largest one among the greatest producers of fish farming with an increasing of 47.5%. Still in São Paulo, Ilha Solteira reservoir is one of the top ten greatest producers of tilapia (*Oreochromis niloticus*) in caged-culture in Brazil [4].

The identification of environmental issues due to the cage-cultured in reservoirs is a challenge because the production is carried out on a small scale. Unsustainable practices in fish farming are related to significant harm potential to aquatic biodiversity and function of the ecosystem [5, 6]. The fish farms located in flooded areas of reservoirs are also subject to anthropic impacts [7].

In aquatic studies, the use of remote sensors have been widely considered and expanded to aquaculture monitoring [8, 9, 10, 11]. One parameter of water quality routinely measured is the water transparency, obtained through the Secchi disk depth (Z_{SD} – in meters). Z_{SD} is an inverse measure of light intensity with depth and, therefore, is a property of primary production in water column. As a result of low Z_{SD} the dissolved oxygen concentration decreases and eutrophication processes increases [9]. Spatial and temporal Z_{SD} derived from remotely sensed data can help to identify critical Z_{SD} values for fish farms [12].

This work aimed to map the water transparency in caged-fish farm from space and to evaluate the short-term impact of this activity on eutrophication.

2. MATERIALS AND METHODS

2.1. Study Area

Fish farms located in the Paranaíba and Grande Rivers tributaries (Formoso, Cupins e Cãn Cãn), located upstream of Ilha Solteira reservoir (Figure 1) were investigated. Cãn Cãn has the greatest fish farm among the other two tributaries, whereas Cupins and Formoso have family-based production. The region climate is the warm tropical (Aw – Köppen) with wet summer and dry winter.

2.2. Land cover mapping

The sub-basins of each tributary selected in this work were obtained using a Digital Elevation Model (DEM). The land cover in these sub-basins was classified using the Normalized Difference Vegetation Index (NDVI) from Landsat-8/OLI images. The selected classes were: water, vegetated and non-vegetated areas. Land cover in situ data were obtained from the AgroTag application, a digital platform for land use and land cover structuration data (*https://agrotag.cnptia.embrapa.br)*. The classification was based on satellite overpass image coincident to first day of fieldwork and applied to season images from 2017 to 2018.

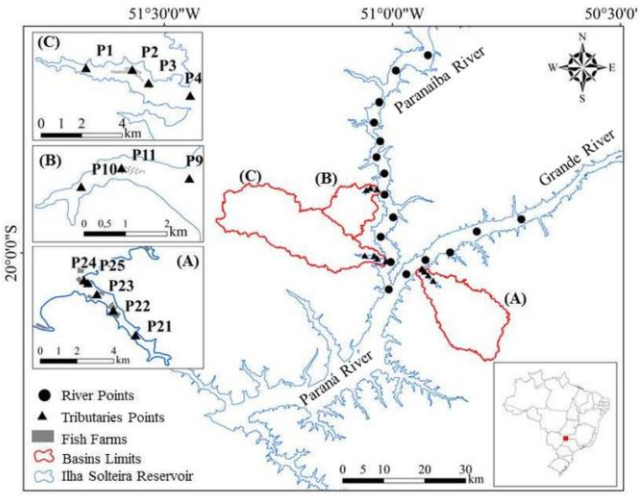

Figure 1. Location of tributaries and basins of (A) Cãn Cãn, (B) Cupins e (C) Formoso with their fish farms and illustration of distribution of sampling points considered in field campaign in Ilha Solteira reservoir.

2.3. In situ data

The fieldwork was carried out from 2 to 5 July 2018. The sampling points in Paranaíba and Grande rivers were determined from stratified sampling technique [13], generating 19 samples. The sampling points in the tributaries were distributed in one point before the fish farms, one point inside the fish farms (between the fish cage) and one after the fish farms and nearest the river. In Formoso, P2 and P3 were collected in the fish farm; in Cupins, was P11, and in Cãn Cãn, P22, P23 and P25 correspond to fish farms.

Above water, reflectance data were collected from hyperspectral spectroradiometer FieldSpec4 (Malvern Panalytical, Almelo, Holanda) between 10:00h and 15:00h of local time (GMT-3) with adequate acquisition geometry to avoid the sun glint effect [14]. The Z_{SD} data were taken using a Secchi disk; water samplings were collected at subsurface to obtain the chlorophyll-*a* ([Chl-*a*]) and total suspended solid ([TSS]) concentrations [15, 16]. Were also measured turbidity, surface temperature and dissolved oxygen (DO) using YSI probe (650 MDS) in the first 30 cm and the depth of each sampling was measured using a deep meter.

2.4. Developing of a regional Z_{SD} model

A wide range semi-analytical algorithm to estimate the Z_{SD} [17] was tested, however, did not achieve satisfactory results. Because of that, we used the empirical approach in order to adjust an algorithm to estimate the Z_{SD}. The in situ hyperspectral reflectance data were firstly simulated for Landsat-8/OLI spectral bands [18]; several combinations between Z_{SD} along the rivers (n = 19) and reflectance ratios were performed to find the most suitable algorithm. The band ratio 443/655 nm achieved a coefficient of correlation of r = 0.82 ($p < 0.001$), therefore, the following algorithm was fitted:

$$Z_{DS} = -4.43 + 8.36 \times \left(\frac{R443}{R665}\right) \quad (1)$$

The Z_{SD} algorithm was applied to a time series of Landsat-8/OLI images, level 2 (surface reflectance - by the Landsat Surface Reflectance Code (LaSRC)) from 2017 to 2018 obtained in U.S. Geological Survey platform (*http://earthexplorer.usgs.gov/*). The months of February, March, July and September were chosen to represent the Austral summer, autumn, winter and spring seasons, respectively. The image selection criterion was based on clouds free over the water bodies. The satellite overpass the study area was coincident to the first day of fieldwork.

3. RESULTS AND DISCUSSION

3.1. Study area characterization

The land cover showed similarity among the basins in season of 2017-2018 (Figure 2). From the land surveys, it was observed grazing land, planted forest and sugarcane in expansion in region, with predominance of the former. The vegetation areas presented reduction in spring and increasing in autumn season due to sugarcane production cycle dynamic. The non-vegetated areas correspond to bare soil and constructed areas.

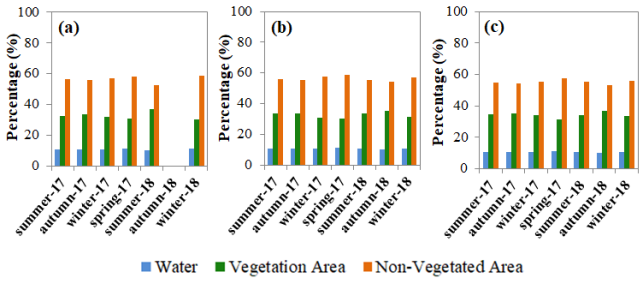

Figure 2. Percentage of land cover of basins of tributaries (a) Cãn Cãn (with Autumn-2018 missing due to clouds cover over the basin), (b) Cupins e (c) Formoso in relation to water, vegetation and non-vegetated classes during the seasons in 2017-2018 period.

In relation to collected data in tributaries, the reflectance spectra revealed a peak at green spectral region (500-600 nm) and slightly absorption at 680 nm, associated to presence of Chl-*a* pigment. The characteristic feature of vegetation related to Chl-*a* was observed at "red edge", with increasing of reflectance at 689 nm (Figure 3). Formoso presented the highest reflectance values among the others, followed by Cupins e Cãn Cãn; the latest registered the highest concentrations of optical significant substances (OSS), Chl-*a* e TSS, and lowest values of Z_{SD}. The tributaries presented reflectance features according to the

rivers where they belong. The lowest reflectance values were observed in sampling points in the fish farms.

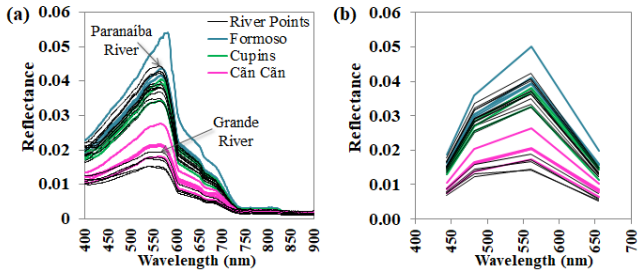

Figure 3. (a) Reflectance spectral curves collected in tributaries and Paranaíba and Grande rivers (sampling spectra highlighted by arrows) and (b) simulated reflectance for center bands (443, 482, 561 and 655 nm) of OLI sensor.

[Chl-*a*] averages were 4.6 ± 3.0 μ L^{-1} in rivers and 3.6 ± 1.5 μ L^{-1} in tributaries (Table 1). In sampling points in fish farms, P2 and P3 in Formoso presented [Chl-*a*] of 4.54 and 2.46 μ L^{-1}; P11 in Cupins had [Chl-*a*] of 4.66 μ L^{-1}; P22, P23 and P25 showed [Chl-*a*] of 4.40, 5.45 and 5.29 μ L^{-1}, respectively.

In fish farms, the fish feed causes nutrients increasing in water, which promotes the algal proliferation and increasing of [Chl-*a*]. The light in water column is more attenuated with [Chl-*a*] increasing and fishes start to compete for oxygen in the confined space of cages. Table 1 shows decreasing of DO in depth (5.2 ± 0.7 mg L^{-1}) in relation to surface (6.4 ± 0.7 mg L^{-1}) and reduction in relation to sampling points along the rivers (7.6 ± 0.2 mg L^{-1}). The surface temperatures were similar between the tributaries and rivers. The average Z_{SD} in tributaries (5.2 ± 0.8 m) was near of Z_{SD} values in rivers (5.4 ± 0.9 m). In Formoso, P2 and P3 presented Z_{SD} of 3.3 and 4.47; Cupins had P11 = 5.5 m and Cãn Cãn showed P22 = 5.56 m, P23 = 5.10 m and P25 = 4.8 m. The turbidity was higher in tributaries than in rivers. [TSS] in tributaries was 0.7 ± 0.4 mg L^{-1} and 0.9 ± 0.5 mg L^{-1}. The high rates of non-vegetated areas in tributaries basins facilitate the entry of terrestrial material into the water bodies. The relationship between [Chl-*a*] and Z_{SD} is exponential (Figure 4); higher the [Chl-*a*] lower the Z_{SD}.

Table 1. Descriptive statistics of water quality data. Turb. = turbidity; Temp. = temperature; Avg. = average; S.D. = standard deviation, Min. = minimum; Max. = maximum.

		Z_{SD} (m)	Depth (m)	Turb. (NTU)	Temp. (°C)	DO (mgL^{-1})		[Chl-*a*]	[TSS]
						Surface	*Depth*	(μ L^{-1})	(mgL^{-1})
River Points *n* =19	*Min-Max*	4.3-7.0	7.9-38.9	2.4-3.8	24.3-25.5		6.8-7.9	0.4-13.8	0.0-1.7
	Avg.± *S.D.*	5.4 ± 0.9	24.6 ± 8.7	3.1 ± 0.4	24.8 ± 0.4		7.6 ± 0.2	4.6 ± 3.0	0.9 ± 0.5
Tributary Points *n* = 12	*Min-Max*	3.8-7.0	8.5-37.3	1.1-7.0	23.5-25.2	5.4-7.7	4.3-6.2	0.8-5.5	0.3-1.6
	Avg.± *S.D.*	5.2 ± 0.8	16.0 ± 8.5	4.2 ± 2.6	24.5 ± 0.5	6.4 ± 0.7	5.2 ± 0.7	3.6-1.5	0.7 ± 0.4

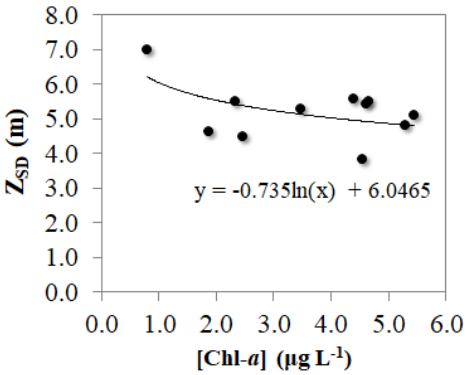

Figure 4. Z_{SD} plotted against [Chl-*a*] for sampling points of tributaries with one point missing of [Chl-*a*] (n = 11).

3.2. Z_{SD} seasonal mapping

The Z_{SD} algorithm presented MAPE (Mean Absolute Percentage Error) of 17.5% (Figure 5) and had better adjustment for Formoso and Cãn Cãn (in situ Z_{SD} average of 4.8 and 5.1 m, respectively) than Cupins (Z_{SD} average of 6.0 m). The use of ratio between blue and red bands works for the study environment and can be explained by the Chl-*a* absorption on these spectral regions.

In Z_{SD} mapping the sampling points located in Formoso presented constancy along the seasons with the highest values in sampling points after the fish farms. In Cupins, the values stayed nearest to minimum values (3.8 m), with the lowest value in the fish farm and highest in adjacent sampling points. Cãn Cãn presented the highest variation with Z_{SD} nearest to maximum values, with lower values in fish farms than outside them.

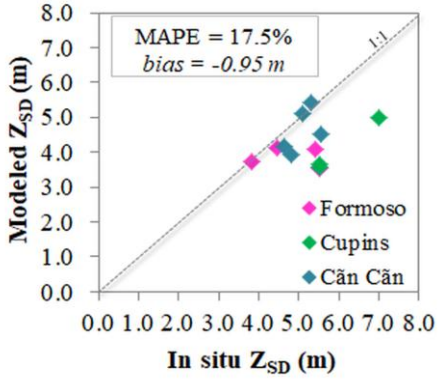

Figure 5. Comparison between estimated Z_{SD} via linear regression model and in situ Z_{SD}.

In Figure 6, Z_{SD} minimum values were found in summer and autumn seasons in all tributaries. Cãn Cãn presented high values in summer-2018 (7.0 m) with reduction on areas with less depth. Cupins and Formoso presented lowest values in fish farms points in relation to Cãn Cãn (3.8 m and 5.0 m, respectively). In winter seasons, with rainfall decreasing, Z_{SD} remained near the maximum

values. In spring-2017, the highest variations were observed. In summary, Z_{SD} values were higher in dry seasons (winter and autumn) than in wet seasons (summer and spring).

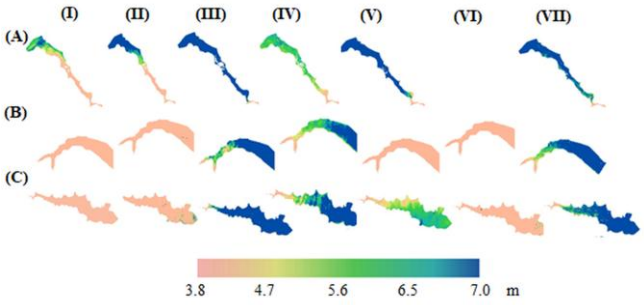

Figure 6. Spatial distribution of Z_{SD} estimations in Formoso (A), Cupins (B) e Cãn Cãn (C) during seasons (I – summer-2017; II – autumn-2017; III – winter-2017; IV – spring-2017; V – summer-2018; VI – autumn-2018; VII – winter-2018).

The input of external material of erosive processes promoted by the bare soil in the basins (non-vegetated area represents about of 55%) and accelerated by rainfall cause the increasing of turbidity and reduction of water transparency.

5. CONCLUSIONS

The water transparency in fish farms in Ilha Solteira reservoir is affected by algal presence. Z_{SD} was useful as an indicator of eutrophication in fish farms and an important parameter to monitoring water quality integrated to remote sensing data. The Z_{SD} short-term analysis showed that the fish farming, considering Chl-*a*, does not impact the water quality of rivers where they are insert. The robustness of Z_{SD} model can be related to similarities between the tributaries and rivers data in addition to the Landsat-8/OLI potential to monitoring inland waters.

The exploration of simplicity of remote sensing empirical approaches allows the operational monitoring of other aquatic areas with aquaculture in spatial and temporal bases. The data and maps of this study are available on *https://embrapa.br/meio-ambiente/plataforma-abc*.

ACKNOWLEDGMENTS

We would like to thank the Brazilian Corporation of Agricultural Research (EMBRAPA), ABC Platform (Multi-institutional Monitoring of Greenhouse Gases Emission Reduction in Agriculture); the research team of BRSAqua, component project of Environmental Management of Aquaculture (CNPq Project N. 421502/2017-7) and the fish farmers in Formoso, Cupins and Cãn Cãn for their welcome of survey team.

6. REFERENCES

[1] EMBRAPA (2016). Aquicultura brasileira cresce 123% em dez anos.https://embrapa.br/busca-de-noticias/-/noticia/18797150. Accessed on October 2018.
[2] IBGE. Produção da Pecuária Municipal. v. 43. p. 1-49. 2015.
[3] FAO (2016). The state of world fisheries and aquaculture: Contributions to food security and nutrition for all.
[4] IBGE. Produção da Pecuária Municipal. v. 44. p. 1-51. 2016.
[5] Lynch, A. J. et al. The social, economic, and environmental importance of inland fish and fisheries. *NRC Research Press*. v. 24. p. 115-121. 2015.
[6] Lima Junior, D. P. et al. Aquaculture expansion in Brazilian freshwaters against the Aichi Biodiversity Targets. *Royal Swedish Academy of Sciences*. v. 47. p. 427-440. 2017.
[7] Wetzel, R. G. Limnology: Lake and river ecosystems. *Elsevier Academic Press*. p. 1006. 2001.
[8] Brezonik, P.; Menken, K. D.; Bauer, M. Landsat-based remote sensing of lake water quality characteristics, including chlorophyll and colored dissolved organic matter (CDOM). *Lake and Reservoir Management*. v. 21. p. 373-382. 2005.
[9] Gernez, P. et al. Remote sensing of suspended particulate matter in turbid oyster-farming ecosystems. *Journal of Geophysical Research: Oceans*. v. 119. p. 7277-7294. 2014.
[10] Gernez, P.; Doxaran, D.; Barillé, L. Shellfish aquaculture from space: potential of Sentinel2 to monitor tide-driven changes in turbidity, chlorophyll concentration and oyster physiological response at the scale of an oyster farm. *Frontiers in Marine Science*. v. 4. n. 137. p. 1.15. 2017.
[11] Araújo, C. A. S. et al. Effects of atmospheric cold fronts on stratification and water quality of a tropical reservoir: implications for aquaculture. *Aquaculture Environment Interactions*. v. 9. p. 385-403. 2017.
[12] Gholizadeh, M. H.; Melesse, A. M.; Reddi, L. A comprehensive review on water quality parameters estimation using remote sensing techniques. *Sensors*. v. 16. n. 1298. p. 1-43. 2016.
[13] Rodrigues, T. W. P. et al. Delineamento amostral em reservatórios utilizando imagens Landsat-8/OLI: um estudo de caso no reservatório de Nova Avanhadava (estado de São Paulo, Brasil). *Boletim de Ciências Geodésicas*. v. 22. n. 2. p. 303-323. 2016.
[14] Mobley, C. D. Estimation of the remote-sensing reflectance from above-surface measurements. *Applied Optics*. v. 38. p. 7442-7455. 1999.
[15] Golterman, H. L.; Clymo, R. S.; Ohnstad, M. A. M. Methods for physical and chemical analysis of fresh water. *Oxford: Blackwell Scientific*. p. 214. 1978.
[16] APHA. American Public Health Association. Standard methods for the examination of water and wastewater. p. 20. 1998.
[17] Lee, Z.P. et al. A semi-analytical scheme to estimate Secchi-disk depth from Landsat-8 measurements. v. 177. p. 101-106. 2016.
[18] Barsi, J. A. et al. The spectral response of the Landsat-8 Operational Land Imager. *Remote Sensing*. v. 6. p. 10232-10251. 2014.